COMMUNICATION

5-Thiaporphyrinium Cation: Effect of Sulphur Incorporation on Excited State Dynamics

Received 00th January 20xx,
Accepted 00th January 20xx

DOI: 10.1039/x0xx00000x

Aashi Takiguchi, [a] Naoto Inai, [b] Seongsoo Kang, [c] Masaya Hagai, [d] Seokwon Lee, [c] Takeshi Yanai,*[b,e] Dongho Kim*[c] and Hiroshi Shinokubo*[a]

We synthesised thionium-ion embedded aromatic porphyrinoids: a free-base 5-thiaporphyrinium cation and its zinc complex. The sulphur atom effectively participates in the macrocyclic π-conjugation. Fluorescence quantum yields of thiaporphyrinium cations were lower than 1% unlike oxaporphyrinium cations. Detailed photophysical analysis and DFT calculations clarified the vibrational mode regarding the out-of-plane motion of the sulphur atom induced ultrafast quenching of the excited state in comparison to the corresponding oxaporphyrinium cations.

Sulphur-containing π-conjugated molecules have rich chemistry. Various applications have been explored to utilise attractive properties from the electronic structures of chalcogens.[1–6] Sulphur atoms are often embedded in aromatic π-systems in five-membered rings such as thiophene derivatives. Thiophene is a 6π aromatic system, which substitutes for a benzene ring structure without inducing charges. In contrast, introducing sulphur in a six-membered ring without disrupting the aromaticity generates a positive charge in a thiopyrylium cation structure. The incorporation of positive charges into heteroatom-containing π-conjugated molecules drastically changes the electronic structure. However, their inherent high reactivity often results in difficult isolation. Consequently, thionium ion-embedded π-conjugated molecules have been less explored than the thiophene embedded counterparts.[7,8]

The sulphur substitution strategy is also valid for porphyrin derivatives. Various sulphur-embedded porphyrins have been synthesised[9–13] such as core-modified porphyrins, dithiaporphyrins and thiacorroles (Fig 1). Those sulphur embedded porphyrins are electrically neutral. Thionium ion incorporated porphyrins, 5-thiaporphyrinium cations, were synthesised around 1970.[14–16] Unfortunately, their instability hampered complete characterization and further investigation.

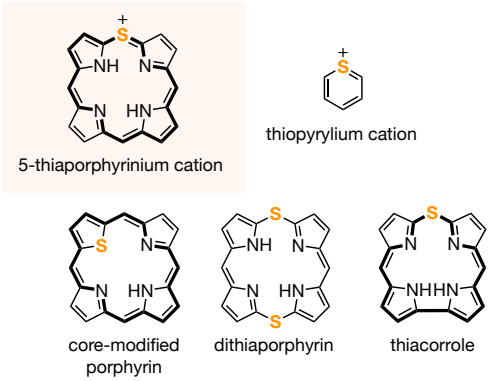

Fig. 1 Sulphur-containing porphyrin derivatives.

Macrocyclic conjugation depends on the types of sulphur insertion. The sulphur atom in the core-modified porphyrins does not directly participate in the macrocyclic conjugation. Dithiaporphyrins and thiacorroles are porphyrinoids with sulphur at the *meso*-position. However, their conjugation patterns are different from regular porphyrins. 5-Thiaporphyrinium cations retain the porphyrin skeleton, in which the sulphur atom directly participates in the macrocyclic conjugation.

In this work, we synthesised stable 5-thiaporphyrinium cations, which are regarded as π-expanded thiopyrylium cations. Here, we disclose the aromaticity and excited state dynamics of the 5-thiaporphyrinium cations to compare with those of the corresponding 5-oxaporphyrinium cations. Our findings shed light on the effect of sulphur insertion into the porphyrin skeleton.

The synthetic route for thiaporphyrinium cations is shown in Scheme 1. Nucleophilic addition of **1-Zn**[17] by sodium sulfide

[a] Department of Molecular and Macromolecular Chemistry, Graduate School of Engineering, Nagoya University, Chikusa-ku, Nagoya, Aichi 464-8603, Japan. E-mail: hshino@chembio.nagoya-u.ac.jp
[b] Department of Chemistry, Graduate School of Science, Nagoya University, Furo-cho, Chikusa-ku, Nagoya, Aichi 464-8602, Japan. E-mail: yanait@chem.nagoya-u.ac.jp
[c] Department of Chemistry, Spectroscopy Laboratory for Functional π-Electronic Systems Yonsei University, Seoul 03722, South Korea. E-mail: dongho@yonsei.ac.kr
[d] Department of Chemistry, School of Science, Nagoya University, Furo-cho, Chikusa-ku, Nagoya, Aichi 464-8602, Japan.
[e] Institute of Transformative Bio-Molecules (WPI-ITbM), Nagoya University, Furo-cho, Chikusa-ku, Nagoya, Aichi 464-8602, Japan.

† Electronic Supplementary Information (ESI) available: Procedure for synthesis, characterization, optical measurements and theoretical calculations. See DOI: 10.1039/x0xx00000x

and demetallation with aqueous hydrochloric acid provided 19-oxo-1-thioxo-bilin **2**. Among various metal complexes (zinc, nickel, cobalt and silver), the use of zinc complex **1-Zn** afforded **2** in the highest yield (98%). Dehydration condensation of **2** with trifluoromethanesulfonic anhydride and the subsequent anion exchange afforded free-base 5-thiaporphyrinium cation **3-2H** containing ca. 1% of free-base 5-oxaporphynrinium cation **1-2H**. This result indicates that the cyclization reaction proceeded through selective nucleophilic attack of the terminal sulphur atom on the carbonyl group. The plausible reaction pathway is shown in Scheme S1. A trace amount of **1-2H** in the crude product was removed by column chromatography with amino-functionalised silica gel. Treatment of **3-2H** with zinc acetylacetonate furnished zinc(II) 5-thiaporphyrinium cation **3-Zn**. Thiaporphyrinium cations **3-2H** and **3-Zn** were stable in the solution and solid states under ambient conditions. On the contrary, free-base 5-thiaporphyrinium bromide salt was reported to be unstable and insoluble, hampering their complete characterization.[14] The stability of the present 5-thiaporphyrinium cations **3-2H** and **3-Zn** is likely due to the bulky and soft tetraarylborate anion.

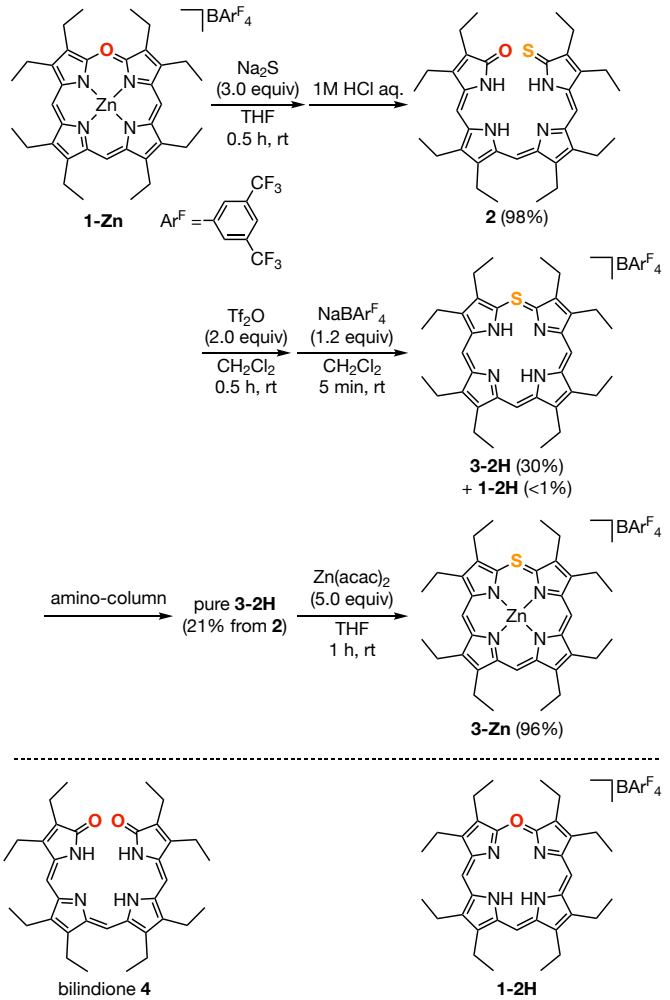

Scheme 1 Synthesis of thiaporphyrinium cations. Ar^F = 3,5-bis(trifluoromethyl)phenyl, Tf$_2$O = trifluoromethanesulfonic anhydride, acac = acetylacetonate.

Single crystal X-ray analysis revealed the structures of **2**, **3-2H** and **3-Zn** (Fig 2). The overall structure of **2** was helical to avoid steric hindrance between carbonyl and thiocarbonyl groups. The positions of three inner NH protons were assigned on the basis of C–N–C bond angles. Thiaporphyrinium cations **3-2H** and **3-Zn** exhibited a planar structure, suggesting sulphur substantially contributed to the macrocycle conjugation. The position of sulphur was disordered at the four *meso*-positions.

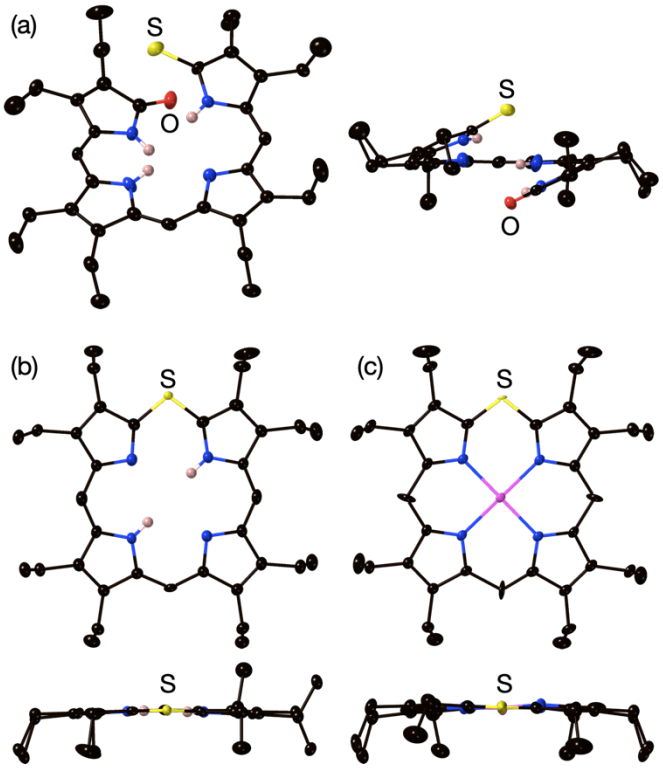

Fig. 2 X-ray crystal structures with thermal ellipsoids drawn at 50% probability. C–H protons and tetraarylborate anions are omitted for clarity. (a) Overall and side views of 2, (b) top and side views of **3-2H**, and (c) top and side views of **3-Zn**.

The *meso* protons in thiaporphyrinium cation **3-2H** appear at 10.26 and 10.24 ppm (Fig S3, ESI†), which are downfield-shifted compared with those of oxaporphyrinium cation **1-2H** (9.41 and 9.05 ppm).[18] In contrast, the inner-NH protons of **3-2H** (–1.05 ppm) were upfield shifted compared with those of **1-2H** (3.28 ppm).[18] A similar trend was also observed between thiopyrylium cation and pyrylium cation.[19] These shifts imply thiaporphyrinium cation **3-2H** possesses a stronger ring current effect than oxaporphyrinium cation **1-2H**. The NICS values and ACID plot support the stronger diatropicity of **3-2H** (Table S6 and Fig S20, ESI†).

Electrochemical potentials of **2**, **3-2H** and **3-Zn** were measured using cyclic voltammograms (Fig S14, ESI†). Free-base thiaporphyrinium cation **3-2H** exhibited one reversible oxidation wave at 1.23 V and two reversible waves at –0.65 V and –1.21 V, which were positively shifted compared with those of free-base oxaporphyrinium cation **1-2H** (oxidation potential: 1.08 V, reduction potential: –0.74 V).[18] The difference would be derived from the larger electron affinity of sulphur than oxygen. A similar tendency was observed in the

oxidation potential of zinc complexes (**3-Zn**: 0.79 V, **1-Zn**: 0.71 V).[17] The oxidation and reduction potentials of zinc thiaporphyrinium cation **3-Zn** at 0.79 V and –0.98 V, respectively, were negatively shifted in comparison to free-base **3-2H**.

The optical spectra of **2**, **3-2H** and **3-Zn** exhibited the effect of sulphur insertion. The UV/Vis/NIR absorption spectrum of **2** was red-shifted to ca. 860 nm compared to that of **4** (Fig 3 (a)). Time-dependent density-functional theory (TD-DFT) calculations suggested that the bathochromic shift in **2** is derived from narrower π–π* transition owing to stabilised LUMO and LUMO+1 by the sulphur atom (Fig S15, S17, and Table S2, ESI†). Whereas oxaporphyrinium cation **1-2H** showed complex Q-like bands due to the presence of *cis*- and *trans*-NH tautomers,[18] the UV/Vis/NIR absorption spectrum of **3-2H** exhibited a simple Q-band (671 nm) (Fig 3 (b)). DFT calculations supported that the *trans*-NH tautomer of **3-2H** is dominant, unlike free-base oxaporphyrinium cation **1-2H**, in which the *cis*-NH tautomer is more energetically stable (Fig S19 and Table S5, ESI†). The spectral feature of **3-Zn** resembles **3-2H**. TD-DFT calculations indicate that the excited state of **3-Zn** is derived from π–π* transition without the contribution of orbitals on zinc. The situation is similar to **3-2H** (Fig S16, S18 and Table S3, S4, ESI†).

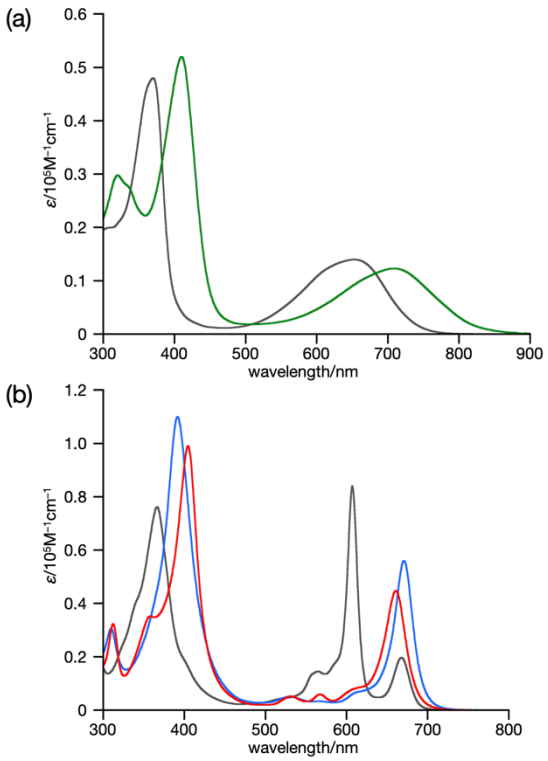

Fig. 3 UV/Vis/NIR absorption spectra in dichloromethane. (a) **2** (green) and **4** (grey). (b) **3-2H** (blue), **3-Zn** (red) and **1-2H** (grey).

Next, we focused on the effect of sulphur on the excited states. Thiaporphyrinium cations **3-2H** and **3-Zn** emitted very weak fluorescence. Both quantum yields were lower than 1%, whereas those of oxaporphyrinium cations **1-2H** and **1-Zn** were 1.7% and 27%, respectively. The fluorescence peaks of thiaporphyrinium cations exhibited almost no enhancement at 77 K without detection of phosphorescence, while those of oxaporphyrin were significantly increased (Table 1). These results suggest that low quantum yields of thiaporphyrinium cations were not explained due to phosphorescence.

Table 1 Fluorescence quantum yields of thiaporphyrins and oxaporphyrins.

	rt[a]	77 K[b,c]
3-2H	<1%	n.d.
3-Zn	<1%	<5%
1-2H	1.7%	40%
1-Zn	27%	56%

[a]solvent: dichloromethane. [b]solvent: 2-methyltetrahydrofuran. [c]Absolute fluorescence quantum yields determined by a calibrated integrating sphere system within ±3% error.

We conducted the time-resolved fluorescence measurements using the time-correlated single photon counting (TCSPC) technique for **1-Zn**, **3-2H** and **3-Zn** in dichloromethane to investigate the effect of sulphur incorporation into the porphyrin skeleton (Fig 4, S21 and S22, ESI†). An excitation pump at 400 nm was employed. **1-Zn** showed decay profiles with a fluorescence lifetime of a few nanoseconds, which is a relatively long-lived component to that of **1-2H**.[18] On the other hand, **3-Zn** showed biexponential decay involving fast fluorescence quenching process with a lifetime of tens of picoseconds, which is followed by a long-lived fluorescence similar to that of **1-Zn**. In the case of **3-2H**, the fluorescence lifetime is too short to observe within the IRF time (30 ps) window of our apparatus. These results imply that the structural rigidification due to zinc metalation in oxa- and thiaporphyrinium cations disrupts the nonradiative decay process.

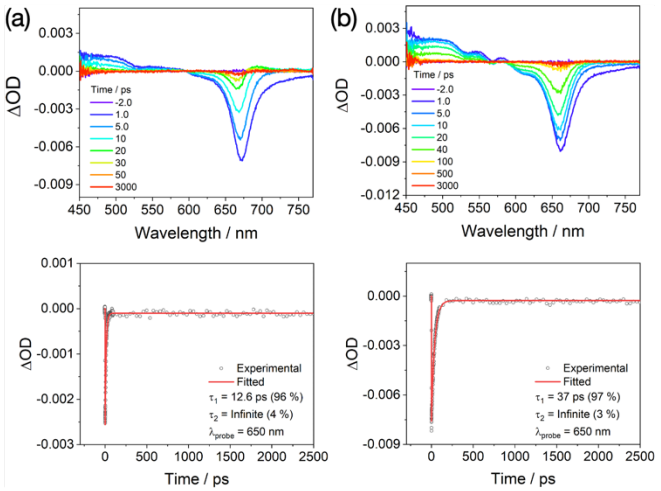

Fig. 4 Femtosecond transient absorption spectra and decay profiles of (a) **3-2H** and (b) **3-Zn** in dichloromethane probed at the visible region. The excitation wavelength of 660 nm is employed.

To get deep insights into the excited-state population dynamics of these porphyrins, we used the femtosecond transient absorption (fs-TA) spectroscopy, where the excitation pump at 660 nm is employed to probe the TA

spectra in the visible region (Fig 4 and S22, ESI†). In all compounds, the TA spectra showed similar ground-state bleaching (GSB) band near 660 nm, which corresponds to the steady-state absorption spectra. The excited-state absorption (ESA) bands were observed below 590 nm with relatively weak band intensities compared with GSB intensities. Compared with the singlet state lifetime of **1-2H** with the time constant of 1 ns,[18] the TA decay profiles of **1-Zn** showed a longer singlet state lifetime over a few nanoseconds (Fig S22, ESI†). This result is well-matched with the fluorescence lifetime obtained by the TCSPC measurements. However, the excited-state dynamics in thiaporphyrinium cations displayed much faster decay profiles than those of oxaporphyrinium cations. Double exponential decay components were obtained in both **3-2H** and **3-Zn**, where initial decay components for **3-2H** and **3-Zn** were fitted in the time constant of 12.6 ps and 37 ps, respectively, followed by the long-lived minor components (Fig 4).

To gain another insight into much faster nonradiative decay in photoexcited thiaporphyrinium cations than oxaporphyrinium cations, we performed theoretical analysis on **1-Zn** and **3-Zn** to simulate their decay rate constants for the electronic- and spin-vibronic transitions from the photoexcited S_1 state (Fig S23–S26 and Table S7, S8, ESI†). The components of the predicted rates suggested that the major decay pathway of photoexcited **1-Zn** should be the intersystem crossing to the T_2 state with a rate constant of 4.7×10^8 s^{-1} (Table S8, ESI†), which is consistent with the previous experimental observation.[18] Meanwhile, the rate constant of the internal conversion to the S_0 state in **3-Zn** was predicted to be 2.1×10^9 s^{-1}, suggesting that the photoexcited **3-Zn** mainly decays through the internal conversion. Further detailed analysis revealed that the remarkable enhancement of the internal conversion decay rate in **3-Zn** is mediated by the lowest-lying vibrational mode associated with the out-of-plane motion of the sulphur atom with a notably low frequency (22.4 cm^{-1}) (Fig S26, ESI†), which is not present in **1-Zn**. This largely-enhanced internal conversion should underlie the small lifetime of the photoexcited thiaporphyrinium cations.

In summary, we synthesised 19-oxo-1-thioxo-bilin **2** as a precursor of thiaporphyrinium cation. We also achieved the synthesis of free-base 5-thiaporphyrinium cation **3-2H**, which was stable under ambient conditions. Complexation of **3-2H** with zinc acetylacetonate afforded zinc(II) 5-thiaporphyrinium cation **3-Zn**. These thiaporphyrinium cations exhibited distinct macrocyclic conjugation from NMR and UV/Vis/NIR spectra. Moreover, detailed optical measurements and theoretical calculations of thiaporphyrins clarified that sulphur insertion into the porphyrinic skeleton accelerated the internal conversion, resulting in low fluorescence quantum yields. The findings would help design bio-active materials based on heteroporphyrins.

There are no conflicts to declare.

Acknowledgements

This work was supported by JSPS KAKENHI grants JP20H05863 (H.S.), JP17H01190 (H.S.), and JP19KK0138 (H.S.). H.S. acknowledges the Sumitomo Foundation for financial support. The work at Yonsei University was supported by the National Research Foundation of Korea (NRF) grant funded by the Korea government (MSIT) (No. 2020R1A5A1019141). A.T. expresses her gratitude for JSPS Research Fellowships for Young Scientists (JP20J11437). A.T. and N.I. thank the "Graduate Program of Transformative Chem-Bio Research" at Nagoya University, supported by MEXT (WISE Program). The authors thank Prof. Dr. Shigehiro Yamaguchi, Dr. Masato Ito, and Ms. Mika Sakai (Nagoya Univ.) for the low-temperature measurement of quantum yield. We also thank Prof. Takashi Ooi and Dr. Yoshitaka Aramaki (Nagoya Univ.) for the fruitful discussion. We express our gratitude to Mr. Takahiro Sakurai (Nagoya Univ.) for the help with X-ray crystallography.

Notes and references

1 M. Stępień, E. Gońka, M. Żyła and N. Sprutta, *Chem. Rev.*, 2017, **117**, 3479-3716.
2 M. E. Cinar and T. Ozturk, *Chem. Rev.*, 2015, **115**, 3036-3140.
3 A. Mishra, C. Q. Ma and P. Bäuerle, *Chem. Rev.*, 2009, **109**, 1141-1276.
4 K. Takimiya, S. Shinamura, I. Osaka and E. Miyazaki, *Adv. Mater.*, 2011, **23**, 4347-4370.
5 X. Guo, M. Baumgarten and K. Müllen, *Prog. Polym. Sci.*, 2013, **38**, 1832-1908.
6 H. F. Yao, L. Ye, H. Zhang, S. S. Li, S. Q. Zhang and J. H. Hou, *Chem. Rev.*, 2016, **116**, 7397-7457.
7 D. Q. Wu, W. Pisula, M. C. Haberecht, X. L. Feng and K. Müllen, *Org. Lett.*, 2009, **11**, 5686-5689.
8 C. H. E. Chow, H. Phan, X. J. Zhang and J. S. Wu, *J. Org. Chem.*, 2020, **85**, 234-240.
9 T. Chatterjee, V. S. Shetti, R. Sharma and M. Rayikanth, *Chem. Rev.*, 2017, **117**, 3254-3328.
10 Y. Matano, *Chem. Rev.*, 2017, **117**, 3138-3191.
11 S. Shimizu, *Heterocycles*, 2020, **100**, 1123-1162.
12 D. Sakow, B. Boker, K. Brandhorst, O. Burghaus and M. Broring, *Angew. Chem. Int. Ed.*, 2013, **52**, 4912-4915.
13 H. Kamiya, T. Kondo, T. Sakida, S. Yamaguchi and H. Shinokubo, *Chem. Eur. J.*, 2012, **18**, 16129-16135.
14 R. L. N. Harris, *Tetrahedron Lett.*, 1969, *10*, 3689-3692.
15 M. J. Broadhur, R. Grigg and A. W. Johnson, *J. Chem. Soc. D*, 1970, 807-809.
16 M. J. Broadhurst, R. Grigg and A. W. Johnson, *J. Chem. Soc., Perkin Trans. 1*, 1972, 1124-1135.
17 A. Takiguchi, E. Sakakibara, H. Sugimoto, O. Shoji and H. Shinokubo, *Angew. Chem. Int. Ed.*, 2022, **61**, e202112456.
18 A. Takiguchi, S. Kang, N. Fukui, D. Kim and H. Shinokubo, *Angew. Chem. Int. Ed.*, 2021, **60**, 2915-2919.
19 G. Doddi and G. Ercolani, *Adv. Heterocycl. Chem.,* 1994, **60**, 65-195.

